Stability of bacterial toggle switches is enhanced by cell-cycle lengthening by several orders of magnitude

Joanna Jaruszewicz,[1] Marek Kimmel,[2,3] and Tomasz Lipniacki[1,4,*]

[1]*Institute of Fundamental Technological Research, Polish Academy of Sciences, 02-106 Warsaw, Poland*

[2]*Departments of Statistics and Bioengineering, Rice University, Houston, Texas 77005, USA*

[3]*Systems Engineering Group, Silesian University of Technology, 44-100 Gliwice, Poland*

[4]*Department of Statistics, Rice University, Houston, Texas 77005, USA*

(Received 27 October 2013; revised manuscript received 14 January 2014; published 11 February 2014)

Bistable regulatory elements are important for nongenetic inheritance, increase of cell-to-cell heterogeneity allowing adaptation, and robust responses at the population level. Here, we study computationally the bistable genetic toggle switch—a small regulatory network consisting of a pair of mutual repressors—in growing and dividing bacteria. We show that as cells with an inhibited growth exhibit high stability of toggle states, cell growth and divisions lead to a dramatic increase of toggling rates. The toggling rates were found to increase with rate of cell growth, and can be up to six orders of magnitude larger for fast growing cells than for cells with the inhibited growth. The effect is caused mainly by the increase of protein and mRNA burst sizes associated with the faster growth. The observation that fast growth dramatically destabilizes toggle states implies that rapidly growing cells may vigorously explore the epigenetic landscape enabling nongenetic evolution, while cells with inhibited growth adhere to the local optima. This can be a clever population strategy that allows the slow growing (but stress resistant) cells to survive long periods of unfavorable conditions. Simultaneously, at favorable conditions, this stress resistant (but slowly growing—or not growing) subpopulation may be replenished due to a high switching rate from the fast growing population.

DOI: 10.1103/PhysRevE.89.022710 PACS number(s): 87.10.Mn, 87.15.A−, 87.16.Yc, 87.17.Ee

I. INTRODUCTION

Epigenetic mechanisms of biological evolution constitute an expanding research area, with important consequences for organism development, proliferative diseases such as cancer, and synthetic biology [1]. A genetic toggle switch, a pair of mutual repressors, is one of the most important circuits introducing bistability to gene regulatory networks [2–5]. Bi- and multistable regulatory elements introduce heterogeneity in cell populations and allow cells in a multicellular organism to specialize and specify their fate. Although multistability is not required for the emergence of coexisting phenotypes [6], decisions between cell death, survival, proliferation, or senescence are likely associated with bistability. In prokaryotes multistability is regarded as an optimal strategy for adapting to varying environmental conditions [7]. Classical examples of toggle switches include the lysis-lysogeny switch in λ phage [8–10], a tetracycline resistance circuit in *Escherichia coli*, Laslo switch in human hematopoiesis [11], several mitogen-activated protein kinase cascades in animal cells [12–14], and cell-cycle regulatory CI circuits in *Xenopus laevis* and *Saccharomyces cerevisiae* [15,16]. Gardner *et al*. [17] constructed a synthetic toggle switch in *E. coli* and provided a theoretical prediction of the conditions sufficient for bistability. Bistability may arise when at least one of the repressors inhibits the competing gene with cooperativity greater than one or when the promoter sites overlap, so the repressors cannot be bound simultaneously [4].

Gene expression in bacterial cells is considered noisy. Stochasticity originating from small numbers of mRNA and protein molecules enables transitions between distinct states. In changing epigenetic landscape noise is favorable as it allows for adaptation; bacteria maximize fitness by tuning noise magnitude with the frequency of the environment fluctuations [18]. The influence of noise on transition rates in a genetic switch has been extensively studied [19–23]. It was shown that the relative stability of the steady states of a toggle as well as of a single autoregulatory gene is controlled by the type of noise [23,24].

In bacteria the average protein lifetime is typically longer than the cell cycle [25], which causes the system to be far from equilibrium. Observations of fast growing *Escherichia coli* cells, which are able to divide as frequently as every 20 min, show an extreme level of cellular activity including continuous reproduction of genome [26], increased number of mRNAs, ribosomal RNAs, and proteins necessary to perform gene expression [27–30]. At high nutrient availability and rapid cell growth DNA elongation rate is roughly constant and DNA replication lasts approximately 40 min [31]; however, at low nutrient levels DNA replication slows down [31,32]. Partitioning of molecules between daughter cells in *E. coli* is binomial [33]. *E. coli* and *B. subtilis* rapidly growing cells are larger than slowly growing cells and can have up to eight origins of replication per cell. However, when the doubling time increases beyond a certain threshold (∼60 min for *B. subtilis*) cell size becomes essentially constant, and cells have at most one replication proceeding [34].

In this article we analyze how the cell-cycle length influences switching rates between two attracting trajectories (epigenetic states) in a bacterial toggle switch. We will consider cell-cycle lengths $T \geqslant 1$ h and assume simultaneous replication of two toggle genes either just before cell division or (in the Appendix A) in the middle of cell cycle. In fact,

*tlipnia@ippt.pan.pl

since DNA replication takes at least about 40 min (in *E. coli*), different genes are present in different copy numbers at a given time of the cell cycle. This effect may have a significant impact on the dynamics of regulatory systems, especially in the case of rapid growth ($T < 1$ h), when genes may have up to eight copies [26,35]. However, in natural systems genes composing a toggle switch (like other regulatory modules) are typically localized in a vicinity of each other [36,37]; see also EcoCyc database [38]. In the case of synthetic toggle switches opposing genes are typically introduced in one plasmid, and therefore replicate in approximately the same time.

II. MODEL

The rate of cell growth and division times are determined by the "housekeeping protein" level, which is assumed proportional to the cell volume $V(t)$. Since there are many genes responsible for protein mass production we assume that the dynamics of the housekeeping protein level is deterministic. Expression of the housekeeping gene is defined by transcription rate constant k_m, translation rate constant k_p, protein degradation rate constant r_p, and mRNA degradation rate constant r_m. Constants k_m and k_p depend on T, while degradation rates r_p and r_m are assumed to be independent of T [28,30]. The cell divides when the housekeeping protein level (or equivalently cell volume) doubles. For simplicity we assume equal assignment of housekeeping protein and its mRNA to progeny cells. Cell growth rate is therefore governed by the housekeeping protein accumulation. Such assumption implies that in the case when no switches occur the concentration of toggle proteins remains roughly constant during the cell cycle.

The housekeeping mRNA $m(t)$ and protein $p(t)$ levels satisfy the following ODEs:

$$\frac{dm}{dt} = k_m - r_m m, \quad \frac{dp}{dt} = k_p m - r_p p, \tag{1}$$

with conditions

$$m(T) = 2m(0), \quad p(T) = 2p(0). \tag{2}$$

The above system has explicit solutions,

$$\begin{aligned} m(t) &= \frac{k_m}{r_m}\left(1 - \frac{1}{e^{r_m t}(2 - e^{-r_m T})}\right), \\ p(t) &= \frac{k_m k_p}{r_m r_p}\left[1 - \frac{1}{r_m - r_p}\left(\frac{r_m}{e^{r_p t}(2 - e^{-r_p T})} - \frac{r_p}{e^{r_m t}(2 - e^{-r_m T})}\right)\right] \quad \text{when} \quad r_m \neq r_p, \\ p(t) &= \frac{k_m k_p}{r_m^2}\left(1 - \frac{1}{e^{r_m t}(2 - e^{-r_m T})}\right) \quad \text{when} \quad r_m = r_p, \end{aligned} \tag{3}$$

where t is the time from the last cell division. The cell volume $V(t) = V_0[p(t)/p(0)]$ [where $V_0 = V(0)$] is therefore given by the expressions

$$V(t) = V_0 + V_0 \frac{r_m(2 - e^{-r_m T})(1 - e^{-r_p t}) - r_p(2 - e^{-r_p T})(1 - e^{-r_m t})}{r_m(2 - e^{-r_m T})(1 - e^{-r_p T}) - r_p(2 - e^{-r_p T})(1 - e^{-r_m T})}, \quad \text{when} \quad r_m \neq r_p, \tag{4}$$

and

$$V(t) = V_0 + V_0 \frac{1 - e^{-r_m t}}{1 - e^{-r_m T}}, \quad \text{when} \quad r_m = r_p. \tag{5}$$

Expressions (4) and (5) imply that $V(T) = 2V_0$, i.e., that the cell doubles its size during the cycle.

We consider a symmetric toggle switch, defined by the continuous time Markov process involving eight random variables: gene 1 and gene 2 states $G_1(t)$, $G_2(t) \in \{0(\text{repressed}),1(\text{active})\}$, numbers of the mRNA 1 and mRNA 2 molecules $M_1(t)$, $M_2(t) \in \mathbb{N}$, numbers of the protein monomer 1 and protein monomer 2 molecules $P_1(t)$, $P_2(t) \in \mathbb{N}$, and numbers of the protein dimer 1 and protein dimer 2 molecules $D_1(t)$, $D_2(t) \in \mathbb{N}$ (Fig. 1). Processes of gene activation, repression, mRNA transcription, protein translation, dimer formation, and dissociation are explicitly included in the model. Propensities of the second-order (bimolecular) reactions are assumed inversely proportional to $V(t)$. We assume that the nutrient level influences the synthesis of the two toggle proteins P_1 and P_2 in the same way as it affects the housekeeping protein synthesis. We assume that the toggle mRNAs transcription rate constants equal k_m and toggle proteins translation rate constants equal k_p.

Here, we will assume that the gene replication takes place just before division; the case in which gene replication takes place in the middle of cell cycle is considered in the Appendix A and leads to similar results. DNA replication

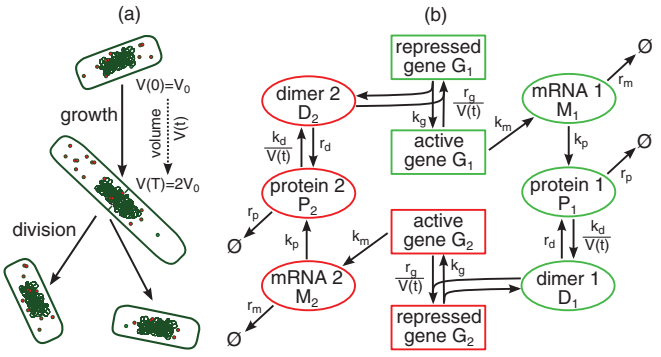

FIG. 1. (Color online) Schematic of the toggle switch model in dividing cells. (a) Schematic of the cell growth and division. (b) Schematic of the toggle switch system.

TABLE I. Reaction-rate constants.

Reaction	Symbol	Default value, $V(t)=1$, $k_m=\bar{k}_m, k_p=\bar{k}_p$	Parameter range for bacteria (vol. 1 μm^3)
Gene repression by protein dimer binding	$k_g/V(t)$	10^{-2}	[a]
Gene activation by protein dimer unbinding	r_g	2×10^{-3}	[a]
mRNA transcription from the active gene	k_m	5×10^{-3}	$\leqslant 0.8$[1/s][b]
Protein translation	k_p	10^{-2}	$\sim10^{-2}$–~10[1/s][c]
Dimer formation	$k_d/V(t)$	5×10^{-4}	1.6×10^{-6}–9.5 [1/(mlcl s)][d]
Dimer dissociation to monomers	r_d	10^{-1}	5×10^{-8}–1.9×10^{3} [1/s][e]
mRNA degradation	r_m	3×10^{-3}	10^{-2}–6×10^{-4}[1/s][f]
Protein monomer degradation	r_p	3×10^{-5}	$\sim1.4\times10^{-5}$–$\sim10^{-2}$ [1/s][g]

[a]Gene switching is causing mRNA bursts observed at an *E. coli* promoter [33].

[b]For *E. coli* maximal transcription rate: 0.16–0.84/s [46].

[c]Translation initiation intervals are of the order of seconds, although they are specific for each mRNA [47]. *E. coli*: translation initiation rate may vary at least 1000-fold [48]; examples of translation initiation frequencies: β-galactosidase—0.31/s (spacing between ribosomes: 110 nucleotides), galactoside acetyltransferase—0.06/s (spacing between ribosomes: 580 nucleotides) [46]; maximal peptide chain elongation rate: 20 aa/s [49,50]; average peptide chain elongation rate: 12 aa/s [46].

[d]All cell types: 9.8×10^{2}/(M s)–5.7×10^{9}/(M s) [51]; for 1 μm^3 volume (bacterial) cell: 1.63×10^{-6}/(mlcl s)–9.47/(mlcl s).

[e]All cell types: 5×10^{-8}/s–1.9×10^{3}/s [51].

[f]The vast majority of mRNAs in a bacterial cell are very unstable, having a half-life of about 3 min (decay rate 3×10^{-3}/s)—bacterial mRNAs are both rapidly synthesized and rapidly degraded [52]. *E. coli*: mRNA half-lives span between 1 and 18 min (decay rates 10^{-2}/s–6×10^{-4}/s) [30].

[g]Most of the bacterial proteins are very stable, with degradation rates: 1.4×10^{-5}–5.6×10^{-5}/s [25]. Some proteins have much higher degradation rates. *E. coli* RNase R has a degradation rate of 10^{-3}/s (in exponential phase) [53]; factor σ^{32} a has degradation rate of 10^{-2}/s (in steady-state growth phase) [54].

requires that the two DNA strands separate and become accessible to DNA polymerase, and therefore leads to dissociation of DNA-bound proteins near the replication forks. Accordingly, we assume that repressor molecules dissociate from DNA leading to gene activation. However, when the repressor level is high the gene may become repressed almost immediately after the replication fork passes that gene. The mRNA, protein monomer, and protein dimer molecules are distributed between daughter cells in one of two ways: (1) following the binomial distribution with parameter 0.5 so that each molecule has equal probability to enter each of the daughter cells, or (2) almost evenly such that the daughter cells both receive half of the molecules of a given type, or half $\pm1/2$ when the half is not an integer.

The transition propensities, assumed equal for both genes, are

$$\begin{aligned}
&G_i=0\to G_i=1, \quad k_g(1-G_i),\\
&G_i=1\to G_i=0, \quad r_g d_{3-i} G_i/V(t),\\
&M_i=m_i\to M_i=m_i+1, \quad k_m G_i,\\
&M_i=m_i\to M_i=m_i-1, \quad r_m m_i,\\
&P_i=p_i\to P_i=p_i+1, \quad k_p m_i,\\
&P_i=p_i\to P_i=p_i-1, \quad r_p p_i,\\
&D_i=d_i\to D_i=d_i+1, \quad k_d p_i(p_i-1)/V(t),\\
&D_i=d_i\to D_i=d_i-1, \quad r_d d_i,
\end{aligned} \tag{6}$$

for $i=1,2$.

The assumed reaction-rate constants are listed in Table I. The stochastic trajectories and the central moments of protein distributions were obtained using the Gillespie algorithm [39]. In the deterministic approximation the state of the system is described by eight continuous variables: gene activities $g_1, g_2 \in [0\ 1]$, levels of mRNAs, proteins, and protein dimers m_1, m_2, p_1, p_2, d_1, d_2. Dynamics of the system between cell divisions follows the ODE system:

$$\frac{dg_i}{dt}=k_g(1-g_i)-\frac{r_g}{V(t)}d_j g_i, \tag{7}$$

$$\frac{dm_i}{dt}=k_m g_i-r_m m_i, \tag{8}$$

$$\frac{dp_i}{dt}=k_p m_i-r_p p_i+2r_d d_i-2\frac{k_d}{V(t)}p_i^2, \tag{9}$$

$$\frac{dd_i}{dt}=\frac{k_d}{V(t)}p_i^2-r_d d_i, \tag{10}$$

where $i=1,2$ and $j=3-i$.

The deterministic approximation is accurate only when the characteristic numbers of molecules are large enough to be replaced by the continuous concentrations. For bacteria this condition is never satisfied, and thus deterministic kinetics equations may serve only as a reference for the stochastic simulations; see Fig. 2. Here, the deterministic analysis is applied to define the two attracting trajectories of the system. In nondividing cells these trajectories are replaced by two stable steady states, in which either one or the other gene dominates. As the system is bistable, all deterministic trajectories, except

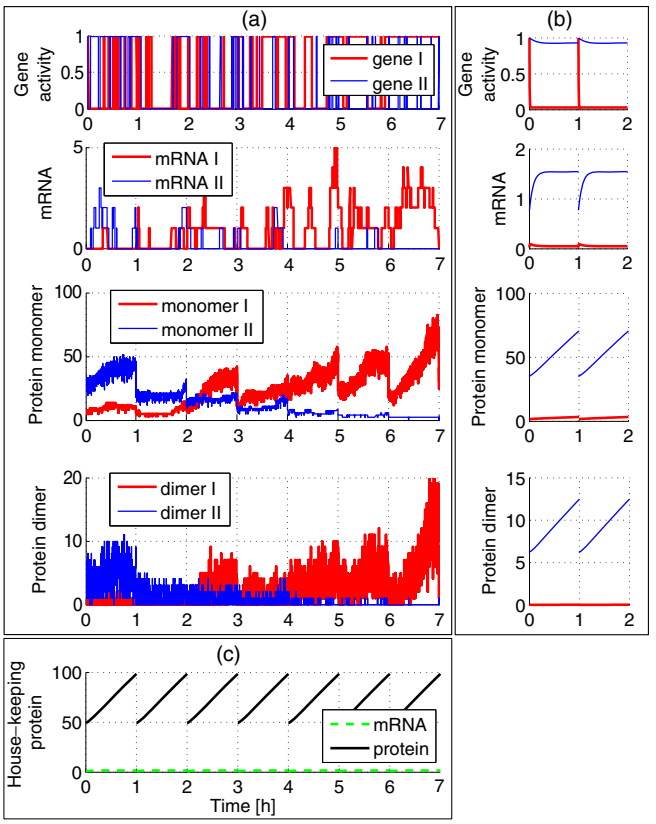

FIG. 2. (Color online) Stochastic (a) and deterministic (b) trajectories of the toggle switch components in dividing cells ($T = 1$ h, binomial distribution of molecules between daughter cells). (c) Deterministic trajectory of the housekeeping protein level controlling cell volume $V(t)$ and divisions.

the separatrix, converge to one of the attracting trajectories; see Fig. 2.

Let p_A and p_I denote protein levels for dominating and dominated gene at the end of the cell cycle, and let d_A and d_I denote corresponding protein dimer levels. Values $p_A(T)$ and $d_A(T)$ increase with T, while $p_I(T)$ and $d_I(T)$ decrease with T and for $T = 1$ h are $p_A = 70.7$, $p_I = 3.4$, $d_A = 12.5$, and $d_I = 0.0$, while for $T = 10$ h are $p_A = 83.3$, $p_I = 2.3$, $d_A = 17.3$, and $d_I = 0.0$.

III. RESULTS

We considered two cases: (I) the transcription rate is constant and the faster protein accumulation and cell growth results from an increase of the translation rate; (II) vice versa, the transcription rate is constant and the translation rate increases. In both cases lengthening of the cell cycle leads to an increase of the mean first passage times (MFPT) between the attracting trajectories. Experimental data suggest that lengthening of the cell cycle is associated with reduced transcription and/or translation rates [28,29].

In case (I), when the transcription rate is kept constant, we found that the MFPT is a sharply increasing function of T, increasing about four orders of magnitude as T increases from 1 h to 60 h; see Fig. 3(a). Moreover, the nondividing and nongrowing cells of constant volume $2V_0$ (the volume of

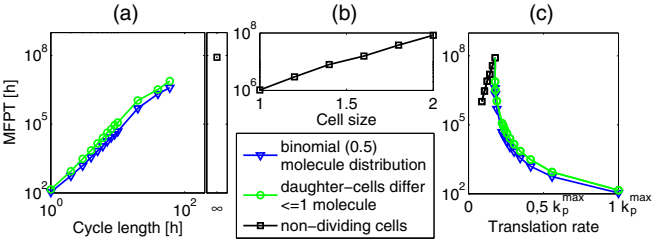

FIG. 3. (Color online) MFPT for the model with the varying protein burst size, case (I). Two types of molecule distributions between sister cells are considered: the most equal (equal in the case of even molecule number; in the uneven case, the one molecule is distributed with probability 0.5 to one of the cells), and binomial with equal probability. The MFPT as function of the cell-cycle length T (a), maximum cell volume in nondividing cells (b), and translation rate (c). For small translation rate cells do not reach volume $2V_0$ and may not divide.

dividing cell just prior to division) have the MFPT six orders of magnitude longer than cells dividing every 1 h; see Fig. 3(a). Cells of constant volume V_0 ($V_0/3$) have the MFPT four (two) orders of magnitude longer than cells dividing every 1 h; see Fig. 3(b). An increase of the cell volume in nondividing cells (in which the translation rate is too small to reach the division size $2V_0$) results in an increase of the MFPT by about two orders of magnitude, as $V(t)$ increases from V_0 to $2V_0$; see Fig. 3(b). As a result, the dependence of the MFPT on the translation rate is a nonmonotonous function; see Fig. 3(c). It increases for small translation rates (for which cells are not able to reach the division volume $2V_0$), and then for dividing cells it rapidly decreases, when an increase of the translation rate shortens T.

In case (II), when the translation rate is kept constant, the MFPT is also an increasing function of T; however, it increases about two orders of magnitude [not four as in case (I)] as T increases from 1 h to 60 h; see Fig. 4(a). The nondividing and nongrowing cells of constant volume equal $2V_0$ (V_0) have the MFPT about 300 (30) times longer than cells dividing every 1 h; see Fig. 4(a). An increase of cell volume in nondividing cells results in approximately 10-fold increase of the MFPT, as $V(t)$ increases from V_0 to $2V_0$; see Fig. 4(b). As a result, similar to case (I), the dependence of the MFPT on the translation rate is a nonmonotonous function; see Fig. 4(c).

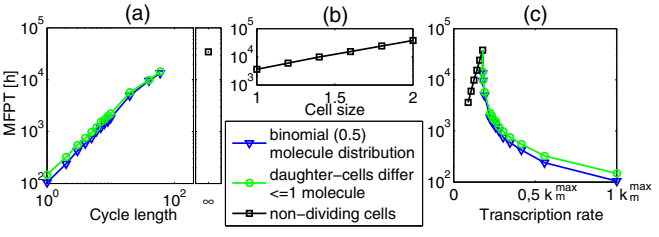

FIG. 4. (Color online) MFPT for the model with constant protein burst size, case (II). The MFPT as a function of the cell-cycle length T (a), maximum cell volume in nondividing cells (b), and transcription rate (c). For small transcription rate cells do not reach volume $2V_0$ and may not divide.

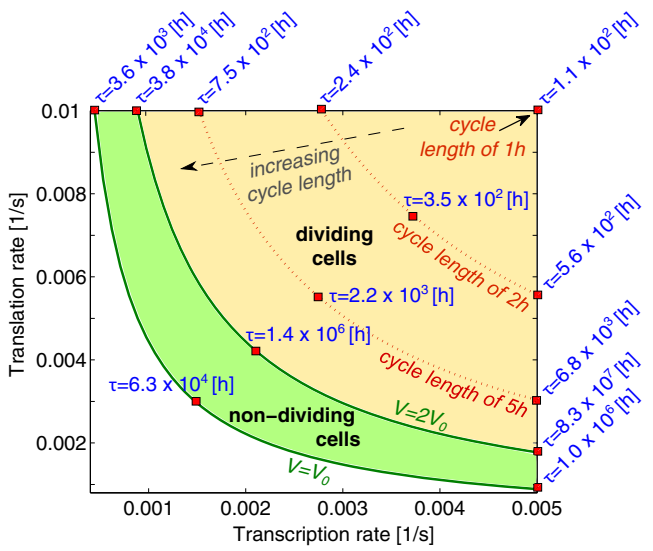

FIG. 5. (Color online) MFPT τ for a varying transcription rate and/or varying translation rate. Cells having small product of transcription and translation rates do not divide and have size between V_0 and $2V_0$.

Interestingly, although the asymmetry in the distribution of molecules leads to shortening of the MFPT, the effect is relatively modest. The ratio of the MFPT when molecule distribution between daughter cells is most symmetric to the MFPT when it is binomial with equal probabilities is less than 2; see Figs. 3 and 4. Assuming that daughter cells are unequal in volume (following a truncated normal distribution with 10% coefficient of variation), which implies unequal probabilities in binomial distributions, we obtained only slightly shorter MFPTs (result not shown).

Dependence of the MFPT on transcription and translation rates for dividing and nondividing cells is summarized in Fig. 5. The effects observed in simulations can be explained as follows. There are two main factors controlling toggling rates [20]: the mean protein number (M) for the dominating gene [roughly proportional to $V(t)$] and the magnitude of noise, which can be measured by the Fano factor (FF = variance/mean), with contributions from the higher moments of the protein distribution in the vicinity of the attracting trajectories. The MFPT was reported to increase exponentially with M [and therefore $V(t)$] [20], and this dependence is seen here for nondividing cells; see Figs. 3(b) and 4(b). Lengthening of the cell cycle is associated with either decrease of the protein burst size $b = k_p/r_m$ (the average number of proteins synthesized from a single mRNA molecule) in case (I), or with a decrease of the mRNA burst size (the average number of mRNA molecules synthesized during the time when the gene is turned on) in case (II). In the considered case a decrease of the protein burst size has a dominant effect on noise as FF $\approx b + 1$ [40,41], and, as a result, on the toggling rates. As shown in Fig. 5, cells having a small translation rate and a correspondingly larger transcription rate (and therefore the same size or the same T) have longer MFPTs. An increase of T [case (I)] associated with a decrease of b leads therefore to a dramatic increase of the MFPT. Moreover, prior to division, cells with longer T have a higher number of proteins associated with the dominating gene and a lower number of proteins associated with the dominated gene, which implies a wider separation of the attracting trajectories. These two effects add to the MFPT elongation with increasing T, and become dominant in case (II), when the elongation of the MFPT (due to the elongation of T) is much smaller than in case (I); see Fig. 3(a) versus Fig. 4(a). In case (II), an increase of the MFPT is also partially attributed to the increase of the mRNA burst size; see Appendix B, Fig. 10.

In Appendix B we analyze numerically the expression of a single gene in dividing cells. We demonstrate that the standard deviation, as well as the third and fourth central moments of the protein distribution, decrease with T. The decrease is substantial (at least twofold, as T changes from 1 to 10 h) in case (I), i.e., with a varied protein burst size, Figs. 8 and 9, or relatively modest (smaller than 25%) in case (II), when the transcription rate varies and protein burst size remains constant; see Figs. 10 and 11.

Finally, we analyze the dynamics of toggle switching process for various T. As shown in Fig. 6, for $T \leqslant 10$ h the transition between the two attracting trajectories is accomplished in four cell cycles (on average). Only in the case of a very long cell-cycle length ($T = 60$ h), the transition is accomplished within the single cell cycle. This effect can be explained as follows. When the cell-cycle length is equal to or shorter than about 10 h (the average protein lifetime) the protein level decreases mostly due to dilution. In such a case after four cell divisions (assuming zero or a very low protein production) the dominating gene protein level may decrease as much as $2^4 = 16$ times and become comparable with the repressed gene protein level enabling state transition. Furthermore, the probability that no protein is produced during cell cycle (or a given number of cell cycles) decreases exponentially with T, which intuitively explains why, in the case when the protein degradation may be neglected, the MFPT increases exponentially with the cell-cycle length T [42]. In nondividing (or very slowly dividing) cells, the protein level decreases (mainly) due to degradation and therefore the above reasoning is no longer valid, and, as demonstrated, the MFPT is controlled by cell size.

IV. CONCLUSIONS

The genetic toggle switch was analyzed theoretically before by several groups, who did not account for the cell cycle. It was found that the lifetimes of toggle states can be very long. Our analysis demonstrates, however, that the stability of the toggle switch dramatically decreases in dividing and fast growing bacteria. Such an effect was experimentally observed in the λ phage toggle switch system in a mutant, $\lambda prm240$, in which the promoter controlling expression of repressor CI is weakened, rendering lysogens unstable [43]. Lysogens grown in minimal medium are stable but switch at high rates when grown in reach medium. For wild type cells, the spontaneous switching rate was almost undetectable, estimated to be equal to 10^{-8}/generation.

Shortening of the cell cycle results from an increase of the translation or transcription rates or both. In the first case (increase of translation) the MFPT was found to be almost six

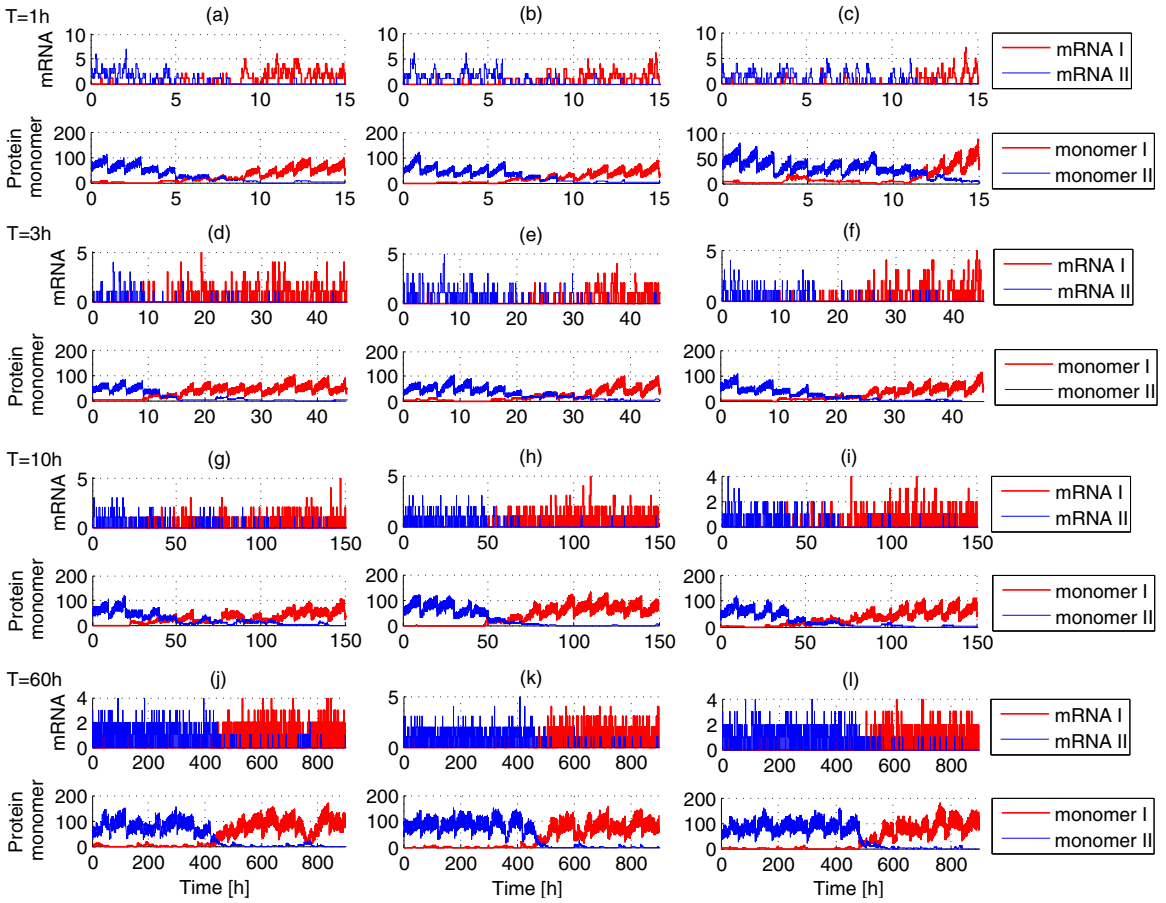

FIG. 6. (Color online) Stochastic trajectories of the toggle switch mRNA and protein monomer numbers in dividing cells with binomial distribution of molecules between daughter cells and (a)–(c) the cell-cycle length $T = 1$ h, (d)–(f) the cell-cycle length $T = 3$ h, (g)–(i) the cell-cycle length $T = 10$ h, and (j)–(l) the cell-cycle length $T = 60$ h.

orders of magnitude shorter for rapidly dividing cells ($T = 1$ h) than for cells with suppressed growth and divisions. We should notice that in these two cases toggle state-to-state transitions are essentially different processes. Nondividing cells remain for most of the time in the tiny vicinity of one of two steady states and the toggling requires transition between these states. In rapidly dividing cells, the system is very far from the equilibrium, i.e., the protein numbers are growing throughout the whole cycle and never approach the vicinity of the steady state. In such a case toggling implies transitions between the two attracting trajectories.

When state-to-state transition is accomplished within one cell cycle (which is the case when the cell cycle is very long) the states of daughter cells remain with large probability the same. However, when cell-cycle length is shorter than the protein degradation time, state-to-state transition requires about four cycles to be accomplished, which allows cells emerging in these four generations to follow divergent trajectories, and may introduce heterogeneity to cell population.

Cell fate and fitness strongly depend on bi- and multistable regulatory elements controlling various aspects of cell behavior. The strong dependence of the MFPT on growth rate has important regulatory consequences. In the case when one state of the toggle is associated with a slow or inhibited growth it automatically becomes much more stable than the opposite state (associated with faster growth). The observation that fast growth dramatically shortens the MFPT and destabilizes the corresponding toggle state suggests that rapidly growing cells vigorously explore the epigenetic landscape enabling nongenetic evolution [1], while cells with slow or inhibited growth adhere to the local optima. From a population perspective this may be an evolutionary optimal strategy. It is known that bacteria and other simple organisms have epigenetic forms, characterized by slower or inhibited growth but higher resistance to environmental stress such as antibiotics treatment, or lack of nutrients [44]. The fraction of cells in the persistent state is determined by state-to-state switching rates as well as growth rates in the persistent and normal states [45]. At favorable conditions the high transition rate from the state of fast growth to the persistent state allow for replenishing the persistent cell population (which tends to be less abundant due to slow or inhibited growth). Simultaneously, the small transition rate from the persistent to normal state enables the persistent cell subpopulation to survive long periods of unfavorable conditions.

ACKNOWLEDGMENTS

J.J. and T.L. were supported by the Foundation for Polish Science Grant TEAM/2009-3/6 and National Science Center

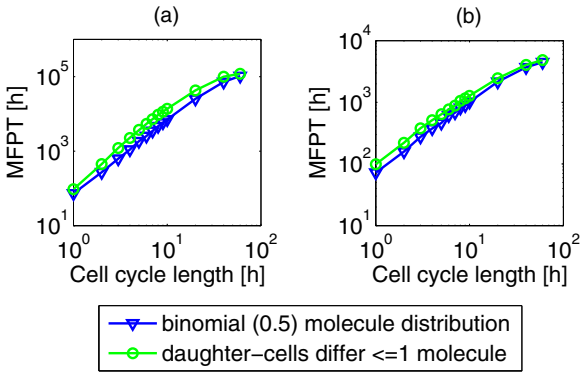

FIG. 7. (Color online) MFPT as a function of the cell-cycle length T for the model with gene replication in $t = 0.5T$. The MFPT for the model with varying protein burst size, case (I) (a), and constant protein burst size, case (II) (b).

(Poland) Grant No. 2011/03/B/NZ2/00281. M.K. was partly supported by the National Science Center (Poland) Grant No. 2012/04/A/ST7/00353. This research was supported in part by PL-Grid Infrastructure. Numerical simulations were carried out at the Zeus computer cluster at the ACK Cyfronet AGH in Cracow, Poland, and at the Grafen computer cluster at the Institute of Fundamental Technological Research in Warsaw, Poland.

APPENDIX A: GENE REPLICATION IN THE MIDDLE OF THE CYCLE

Here, we confirm that the MFPT increases with the cell-cycle length T also when the toggle genes replicate not just before division but earlier during the cell cycle. Namely, we assume that DNA replication takes place in the middle of the cell cycle, i.e., at $t = 0.5T$. To shorten the numerical simulation time, we assume two times smaller translation rate than in the previous case. As already discussed, the translation rate controls the number of protein molecules and therefore toggling rates, which become very long (hard to determine in numerical simulations), when an increase of gene copy number is not compensated by a decrease of translation (or transcription rate). In this model variant in the deterministic approximation the protein monomer and protein dimer levels just before division are $p_A = 53.7$, $p_I = 4.4$, $d_A = 7.2$, and $d_I = 0.0$ (for $T = 1$ h), and $p_A = 65.8$, $p_I = 3.5$, $d_A = 10.8$, and $d_I = 0.0$ (for $T = 10$ h).

In case (I) (constant transcription rate), we found that the MFPT is a sharply increasing function of T, increasing more than three orders of magnitude as T increases from 1 h to 60 h; see Fig. 7(a). In case (II) (constant translation rate), the MFPT increases about 50-fold as T increases from 1 h to 60 h; see Fig. 7(b). The obtained results confirmed that, also for gene replication in the middle of the cell cycle, a decrease in growth rate stabilizes the state of the system; see Fig. 7.

APPENDIX B: SINGLE GENE MODEL WITHOUT AUTOREGULATION IN DIVIDING CELLS

Toggling rates increase with an increasing width of the protein distribution in the vicinity of each of the attracting

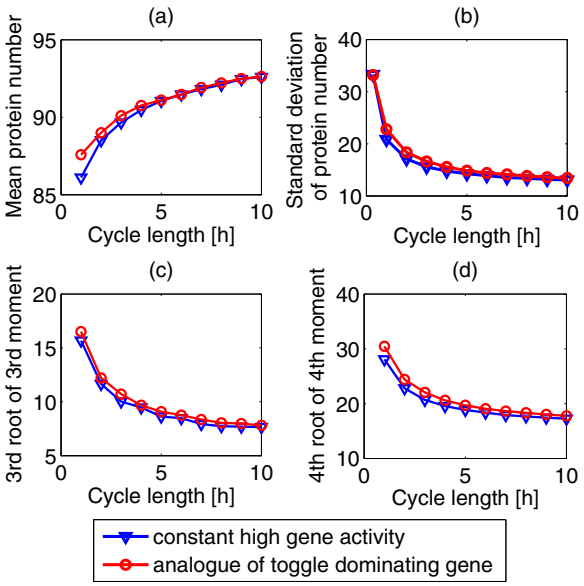

FIG. 8. (Color online) Varied protein burst size [case (I)], analog of the dominating gene. Central moments of the protein distribution just before division. Simulations were performed assuming a binomial molecule distribution, for two cases of gene expression regulation: (1) constant gene activity (blue triangles) and (2) gene switching with rates equal to switching rates of the dominating gene in the toggle (red circles).

trajectories. Here, we investigate how the first four central moments of the protein distribution depend on the cell-cycle length T. Since we are interested in the width of the protein distribution in the basins of the attracting trajectories (not the width of the whole protein distribution, which is controlled mainly by the separation of the attracting trajectories), we consider an expression of a single gene without autoregulation, instead of the toggle switch.

We analyze two models (defining continuous time Markov processes), with and without gene switching. In each model two sets of parameters corresponding to the dominating (Figs. 8 and 10) or dominated (Figs. 9 and 11) gene in the toggle are considered.

In the model without gene switching the state of the system is described by the two random variables: the number of mRNA molecules $M(t) \in \mathbb{N}$ and number of protein molecules $P(t) \in \mathbb{N}$.

The transition propensities are as follows:

$$\begin{aligned} M = m &\to M = m + 1, \quad k_m k_g/(k_g + r_g d_T), \\ M = m &\to M = m - 1, \quad r_m m, \\ P = p &\to P = p + 1, \quad k_p m, \\ P = p &\to P = p - 1, \quad r_p p. \end{aligned} \tag{B1}$$

We assume $d_T = d_A$ or $d_T = d_I$, where d_A and d_I are the mean protein dimer numbers just before division, for dominating and dominated gene, respectively, in the toggle switch model for cells with the cycle length of T. Therefore, the gene activity $k_g/(k_g + r_g d_T)$ is equal to the probability that the toggle gene (dominating or dominated) is active. All other parameters are the same as in the toggle switch model; see Table I. As a

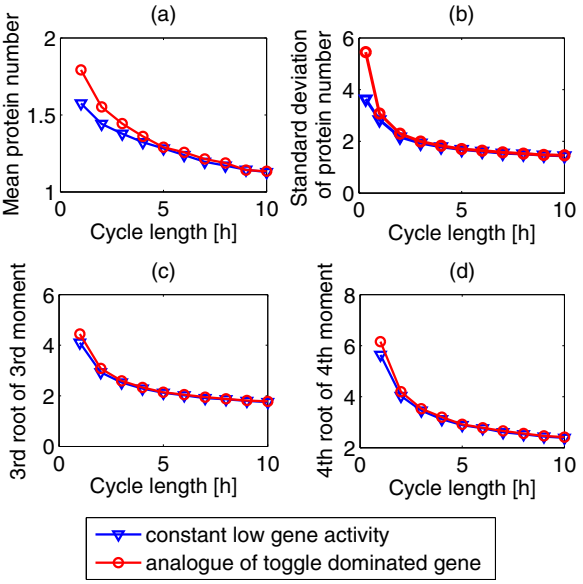

FIG. 9. (Color online) Varied protein burst size [case (I)], analog of the dominated gene. Central moments of the protein distribution just before division. Simulations were performed assuming a binomial molecule distribution, for two cases of gene expression regulation: (1) constant gene activity (blue triangles) and (2) gene switching with rates equal to switching rates of the dominated gene in the toggle (red circles).

result, analogous to the toggle switch system (see main text), the mean protein number before division increases with T for the dominating gene (Figs. 8 and 10), and decreases for the dominated gene (Figs. 9 and 11).

In the model with gene switching, there is an additional random variable, representing the gene state, either active ($G = 1$) or inactive ($G = 0$). In this model the transition propensities are

$$\begin{aligned} &G = 0 \to G = 1, \quad k_g(1 - G), \\ &G = 1 \to G = 0, \quad r_g G d_T, \\ &M = m \to M = m + 1, \quad G k_m, \\ &M = m \to M = m - 1, \quad r_m m, \\ &P = p \to P = p + 1, \quad k_p m, \\ &P = p \to P = p - 1, \quad r_p p. \end{aligned} \tag{B2}$$

We assume $d_T = d_A$ or $d_T = d_I$, where d_A or d_I are the mean protein dimer numbers for dominating and dominated gene, respectively, in the toggle switch model in cells with the cycle length of T. This assumption implies that the gene is switched *on* and *off* with the same rates as either the dominating and dominated gene in the toggle. Analogous to the toggle switch model we will assume that the gene is activated at the division (due to the repressor release during the DNA replication). To determine the influence of this assumption, we also considered the model variant in which the assumption is released; see Figs. 10 and 11.

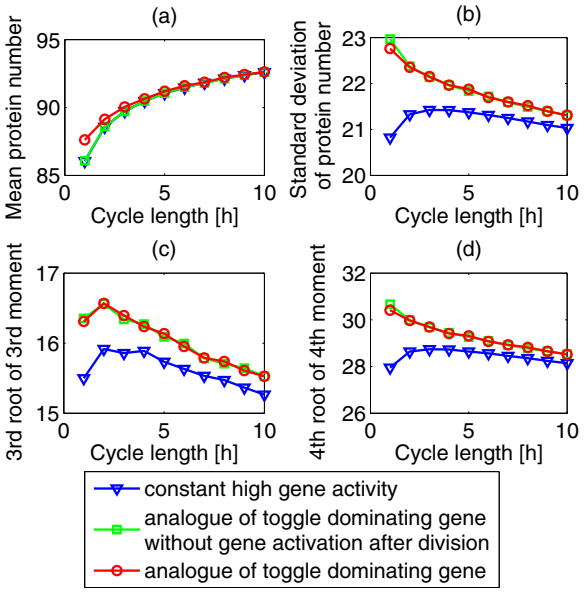

FIG. 10. (Color online) Constant protein burst size [case (II)], analog of the dominating gene. Central moments of the protein distribution just before division. Simulations were performed assuming a binomial molecule distribution, for three cases of gene expression regulation: (1) constant gene activity (blue triangles), (2) gene switching with rates equal to switching rates of the dominating gene in the toggle without gene activation after each division (green squares), and (3) gene switching with rates equal to switching rates of the dominating gene in the toggle (with gene activation after each division) (red circles).

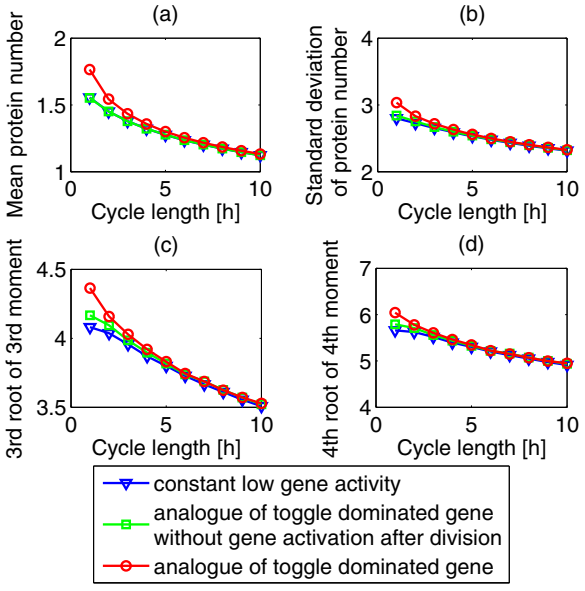

FIG. 11. (Color online) Constant protein burst size [case (II)], analog of the dominated gene. Central moments of the protein distribution just before division. Simulations were performed assuming a binomial molecule distribution, for three cases of gene expression regulation: (1) constant gene activity (blue triangles), (2) gene switching with rates equal to switching rates of the dominated gene in the toggle without gene activation after each division (green squares), and (3) gene switching with rates equal to switching rates of the dominated gene in the toggle (with gene activation after each division) (red circles).

1. Estimation of central moments of the protein distribution

We analyze the following two cases introduced in the main paper.

Case (I), in which an increase of T results from decreases in translation rate (decreasing protein burst size); see Figs. 8 and 9.

Case (II), in which an increase of T results from decreases in transcription rate; see Figs. 10 and 11.

In each case by means of long run multiprocessor simulations we estimate the probability distribution of the protein number at the time of division, and calculate the mean, second, third, and fourth central moments. For each set of parameters we use trajectories having at least 10^5 divisions for Figs. 8 and 9, or 10^7 for Figs. 10 and 11.

a. Case (I): Varied protein burst size

In case (I) the decrease of protein burst size is responsible for a significant decrease of second, third, and fourth central moments of the protein number; see Figs. 8 and 9. This effect was observed and explained previously for nondividing cells, for which the Fano factor of the protein number distribution is proportional to $b + 1$, where b is the protein burst size (protein translation rate divided by mRNA degradation rate) [41]. The similar dependence was obtained many years ago by Otto Berg who calculated the protein number probability distribution in dividing bacteria [40]. In the model with the constant gene activity, there is no contribution from the gene switching noise, and therefore all central moments are smaller than in the model accounting for the gene switching. However, the noise contribution from the gene switching is much smaller than that of the increasing protein burst size.

b. Case (II): Constant protein burst size

In case (II) the size of the protein level fluctuations for the gene corresponding to the dominating gene in the toggle changes with T mostly due to the varying average size of mRNA bursts emerging in periods of gene activity (Fig. 10).

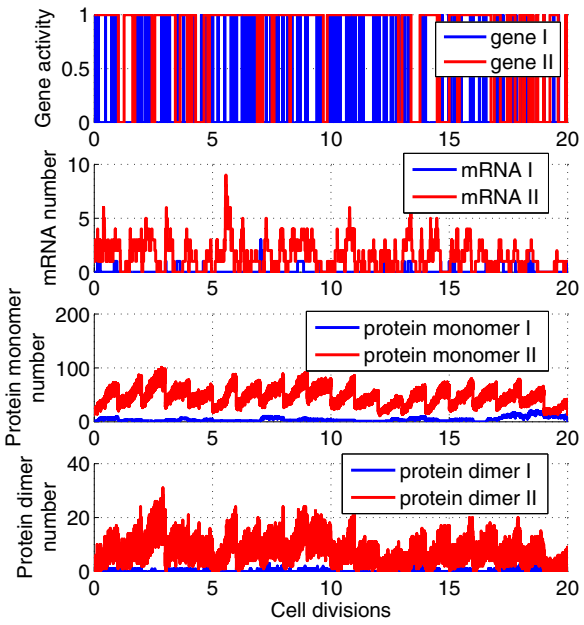

FIG. 12. (Color online) Stochastic trajectory of the toggle switch components in dividing cells. Cell-cycle length $T = 1$ h, binomial distribution of molecules between daughter cells.

This is evident when models with and without gene switching are compared. However, in the case when the analog of the dominated gene is considered the effect of varying size of mRNA bursts is small because the transcription rate is small and the probability that more than one mRNA molecule is synthesized is relatively low. Only for a short cell cycle, $T = 1$ h, can several mRNA molecules be synthesized in short periods of activity of the dominated gene, see Fig. 12, and correspondingly, for a short cell cycle the difference between models with and without gene switching is more pronounced. However, for the analog of the dominated gene the central moments decrease with cell-cycle lengthening simply because the mean protein level decreases.

[1] S. Huang, BioEssays **34**, 149 (2012).
[2] J. E. Ferrell, Jr., Curr. Opin. Cell Biol. **14**, 140 (2002).
[3] T. Tian and K. Burrage, Proc. Natl. Acad. Sci. U.S.A. **103**, 8372 (2006).
[4] A. Lipshtat, A. Loinger, N. Q. Balaban, and O. Biham, Phys. Rev. Lett. **96**, 188101 (2006).
[5] A. Chatterjee, Y. N. Kaznessis, and W.-S. Hu, Curr. Opin. Biotech. **19**, 475 (2008).
[6] R. B. Hoyle, D. Avitabile, and A. M. Kierzek, PLoS Comput. Biol. **8**, e1002396 (2012).
[7] E. Kussell and S. Leibler, Science **309**, 2075 (2005).
[8] M. Ptashne, *A Genetic Switch: Phage λ and Higher Organisms* (Cell Press and Blackwell Scientific Publications, Cambridge, MA, 1992).
[9] A. Arkin, J. Ross, and H. H. McAdams, Genetics **149**, 1633 (1998).
[10] T. Tian and K. Burrage, J. Theor. Biol. **227**, 229 (2004).
[11] P. Laslo, C. J. Spooner, A. Warmflash, D. W. Lancki, H.-J. Lee, R. Sciammas, B. N. Gantner, A. R. Dinner, and H. Singh, Cell **126**, 755 (2006).
[12] J. E. Ferrell and E. M. Machleder, Science **280**, 895 (1998).
[13] U. S. Bhalla, P. T. Ram, and R. Iyengar, Science **297**, 1018 (2002).
[14] C. P. Bagowski and J. E. Ferrell, Jr., Curr. Biol. **11**, 1176 (2001).
[15] J. R. Pomerening, E. D. Sontag, and J. E. Ferrell, Nat. Cell Biol. **5**, 346 (2003).
[16] F. R. Cross, V. Archambault, M. Miller, and M. Klovstad, Mol. Biol. Cell **13**, 52 (2002).
[17] T. S. Gardner, C. R. Cantor, and J. J. Collins, Nature (London) **403**, 339 (2000).
[18] A. S. Ribeiro, Phys. Rev. E **78**, 061902 (2008).
[19] P. B. Warren and P. R. ten Wolde, Phys. Rev. Lett. **92**, 128101 (2004).

[20] P. B. Warren and P. R. ten Wolde, J. Phys. Chem. B **109**, 6812 (2005).
[21] M. Komorowski, J. Miekisz, and A. M. Kierzek, Biophys. J. **96**, 372 (2009).
[22] X. Dai, O. Yli-Harja, and A. S. Ribeiro, Bioinformatics **25**, 2362 (2009).
[23] J. Jaruszewicz and T. Lipniacki, Phys. Biol. **10**, 035007 (2013).
[24] J. Jaruszewicz, P. J. Zuk, and T. Lipniacki, J. Theor. Biol. **317**, 140 (2013).
[25] K. P. Jayapal, S. Sui, R. J. Philp, Y.-J. Kok, M. G. Yap, T. J. Griffin, and W.-S. Hu, J. Proteome Res. **9**, 2087 (2010).
[26] S. Cooper and C. E. Helmstetter, J. Mol. Biol. **31**, 519 (1968).
[27] M. Scott, C. W. Gunderson, E. M. Mateescu, Z. Zhang, and T. Hwa, Science **330**, 1099 (2010).
[28] S. T. Liang, Y. C. Xu, P. Dennis, and H. Bremer, J. Bacteriol. **182**, 3037 (2000).
[29] H. Bremer and P. P. Dennis, *Escherichia Coli and Salmonella* (ASM Press, Washington, DC, 1996), pp. 1553–1569, Chap. 97.
[30] J. A. Bernstein, A. B. Khodursky, P.-H. Lin, S. Lin-Chao, and S. N. Cohen, Proc. Natl. Acad. Sci. U.S.A **99**, 9697 (2002).
[31] O. Michelsen, M. J. T. de Mattos, P. R. Jensen, and F. G. Hansen, Microbiology **149**, 1001 (2003).
[32] M. Bipatnath, P. P. Dennis, and H. Bremer, J. Bacteriol. **180**, 265 (1998).
[33] I. Golding, J. Paulsson, S. M. Zawilski, and E. C. Cox, Cell **123**, 1025 (2005).
[34] M. G. Sargent, J. Bacteriol. **123**, 7 (1975).
[35] M. Osella and M. C. Lagomarsino, Phys. Rev. E **87**, 012726 (2013).
[36] J. Tamames, G. Casari, C. Ouzounis, and A. Valencia, J. Mol. Evol. **44**, 66 (1997).
[37] J. Tamames, Genome Biol. **2**, 0020 (2001).
[38] I. M. Keseler, A. Mackie, M. Peralta-Gil, A. Santos-Zavaleta, S. Gama-Castro, C. Bonavides-Martínez, C. Fulcher, A. M. Huerta, A. Kothari, M. Krummenacker, M. Latendresse, L. Muñiz Rascado, Q. Ong, S. Paley, I. Schröder, A. G. Shearer, P. Subhraveti, M. Travers, D. Weerasinghe, V. Weiss, J. Collado-Vides, R. P. Gunsalus, I. Paulsen, and P. D. Karp, Nucleic Acids Res. **41**, D605 (2013).
[39] D. T. Gillespie, J. Phys. Chem. **81**, 2340 (1977).
[40] O. G. Berg, J. Theor. Biol. **71**, 587 (1978).
[41] M. Thattai and A. Van Oudenaarden, Proc. Natl. Acad. Sci. U.S.A. **98**, 8614 (2001).
[42] C. Zong, L.-h. So, L. A. Seplveda, S. O. Skinner, and I. Golding, Mol. Syst. Biol. **6**, 440 (2010).
[43] J. W. Little and C. B. Michalowski, J. Bacteriol. **192**, 6064 (2010).
[44] N. Q. Balaban, J. Merrin, R. Chait, L. Kowalik, and S. Leibler, Science **305**, 1622 (2004).
[45] D. Nevozhay, R. M. Adams, E. Van Itallie, M. R. Bennett, and G. Balázsi, PLoS Comput. Biol. **8**, e1002480 (2012).
[46] D. Kennell and H. Riezman, J. Mol. Biol. **114**, 1 (1977).
[47] B. S. Laursen, H. P. Sørensen, K. K. Mortensen, and H. U. Sperling-Petersen, Microbiol. Mol. Biol. Rev. **69**, 101 (2005).
[48] L. L. Sampson, R. W. Hendrix, W. M. Huang, and S. R. Casjens, Proc. Natl. Acad. Sci. U.S.A. **85**, 5439 (1988).
[49] R. Young and H. Bremer, Biochem. J. **160**, 185 (1976).
[50] H. Bremer, J. Hymes, and P. P. Dennis, J. Theor. Biol. **45**, 379 (1974).
[51] H. Bai, K. Yang, D. Yu, C. Zhang, F. Chen, and L. Lai, Proteins **79**, 720 (2011).
[52] B. Alberts, A. Johnson, J. Lewis, M. Raff, K. Roberts, and P. Walter, *Molecular Biology of the Cell* (Garland Science, New York, 2002).
[53] G. Chen and M. P. Deutscher, RNA **16**, 667 (2010).
[54] H. El-Samad, H. Kurata, J. C. Doyle, C. A. Gross, and M. Khammash, Proc. Natl. Acad. Sci. U.S.A. **102**, 2736 (2005).